

Selective formation of ultrathin PbSe on Ag(111)

Jing Wang(王静), Meysam Bagheri Tagani, Li Zhang(张力), Yu Xia(夏雨), Qilong Wu(吴奇龙), Bo Li(黎博), Qiwei Tian(田麒玮), Yuan Tian(田园), Long-Jing Yin(殷隆晶), Lijie Zhang(张利杰), and Zhihui Qin(秦志辉)
Citation: Chin. Phys. B, 2022, 31 (**9**): 096801. DOI: 10.1088/1674-1056/ac7867
Journal homepage: http://cpb.iphy.ac.cn; http://iopscience.iop.org/cpb

What follows is a list of articles you may be interested in

Two-dimensional Sb cluster superlattice on Si substrate fabricated by a two-step method

Runxiao Zhang(张润潇), Zi Liu(刘姿), Xin Hu(胡昕), Kun Xie(谢鹍), Xinyue Li(李新月), Yumin Xia(夏玉敏), and Shengyong Qin(秦胜勇)
Chin. Phys. B, 2022, 31 (**8**): 086801. DOI: 10.1088/1674-1056/ac70c1

Surface electron doping induced double gap opening in T_d-WTe_2

Qi-Yuan Li(李启远), Yang-Yang Lv(吕洋洋), Yong-Jie Xu(徐永杰), Li Zhu(朱立), Wei-Min Zhao(赵伟民), Yanbin Chen(陈延彬), and Shao-Chun Li(李绍春)
Chin. Phys. B, 2022, 31 (**6**): 066802. DOI: 10.1088/1674-1056/ac632e

Molecular beam epitaxy growth of monolayer hexagonal $MnTe_2$ on Si(111) substrate

S Lu(卢帅), K Peng(彭坤), P D Wang(王鹏栋), A X Chen(陈爱喜), W Ren(任伟), X W Fang(方鑫伟), Y Wu(伍莹), Z Y Li(李治云), H F Li(李慧芳), F Y Cheng(程飞宇), K L Xiong(熊康林), J Y Yang(杨继勇), J Z Wang(王俊忠), S A Ding(丁孙安), Y P Jiang(蒋烨平), L Wang(王利), Q Li(李青), F S Li(李坊森), and L F Chi(迟力峰)
Chin. Phys. B, 2021, 30 (**12**): 126804. DOI: 10.1088/1674-1056/ac2e63

Phase transition-induced superstructures of β-Sn films with atomic-scale thickness

Le Lei(雷乐), Feiyue Cao(曹飞跃), Shuya Xing(邢淑雅), Haoyu Dong(董皓宇), Jianfeng Guo(郭剑锋), Shangzhi Gu(顾尚志), Yanyan Geng(耿燕燕), Shuo Mi(米烁), Hanxiang Wu(吴翰翔), Fei Pang(庞斐), Rui Xu(许瑞), Wei Ji(季威), and Zhihai Cheng(程志海)
Chin. Phys. B, 2021, 30 (**9**): 096804. DOI: 10.1088/1674-1056/ac11e8

NBN-doped nanographene embedded with five- and seven-membered rings on Au(111) surface

Huan Yang(杨欢), Yun Cao(曹云), Yixuan Gao(高艺璇), Yubin Fu(付钰彬), Li Huang(黄立), Junzhi Liu(刘俊治), Xinliang Feng(冯新亮), Shixuan Du(杜世萱), and Hong-Jun Gao(高鸿钧)
Chin. Phys. B, 2021, 30 (**5**): 056802. DOI: 10.1088/1674-1056/abeede

---

RAPID COMMUNICATION

Selective formation of ultrathin PbSe on Ag(111)

Jing Wang(王静)[1], Meysam Bagheri Tagani[2], Li Zhang(张力)[1,†], Yu Xia(夏雨)[1], Qilong Wu(吴奇龙)[1], Bo Li(黎博)[1], Qiwei Tian(田麒玮)[1], Yuan Tian(田园)[1], Long-Jing Yin(殷隆晶)[1], Lijie Zhang(张利杰)[1], and Zhihui Qin(秦志辉)[1,‡]

[1] *Key Laboratory for Micro/Nano Optoelectronic Devices of Ministry of Education & Hunan Provincial Key Laboratory of Low-Dimensional Structural Physics and Devices, School of Physics and Electronics, Hunan University, Changsha* 410082, *China*
[2] *Department of Physics, University of Guilan, P.O. Box* 41335-1914, *Rasht, Iran*

(Received 7 May 2022; revised manuscript received 29 May 2022; accepted manuscript online 14 June 2022)

Two-dimensional (2D) semiconductors, such as lead selenide (PbSe), locate at the key position of next-generation devices. However, the ultrathin PbSe is still rarely reported experimentally, particularly on metal substrates. Here, we report the ultrathin PbSe synthesized via sequential molecular beam epitaxy on Ag(111). The scanning tunneling microscopy is used to resolve the atomic structure and confirms the selective formation of ultrathin PbSe through the reaction between Ag_5Se_2 and Pb, as further evidenced by the theoretical calculation. It is also found that the increased accumulation of Pb leads to the improved quality of PbSe with larger and more uniform films. The detailed analysis demonstrates the bilayer structure of synthesized PbSe, which could be deemed to achieve the 2D limit. The differential conductance spectrum reveals a metallic feature of the PbSe film, indicating a certain interaction between PbSe and Ag(111). Moreover, the moiré pattern originated from the lattice mismatch between PbSe and Ag(111) is observed, and this moiré system provides the opportunity for studying physics under periodical modulation and for device applications. Our work illustrates a pathway to selectively synthesize ultrathin PbSe on metal surfaces and suggests a 2D experimental platform to explore PbSe-based opto-electronic and thermoelectric phenomena.

Keywords: ultrathin lead selenide (PbSe), scanning tunneling microscopy/spectroscopy (STM/STS), molecular beam epitaxy

PACS: 68.37.Ef, 68.55.–a, 81.15.Hi **DOI:** 10.1088/1674-1056/ac7867

1. Introduction

The ultrathin semiconductor attracts much attention due to the improved performances ranging from electrical properties to optical responses, which is apparent in graphene and transition metal dichalcogenides.[1–4] Lead selenide (PbSe), a representative IV–VI compound, has been extensively studied so far, appearing the noticeable infrared optical response,[5–7] thermoelectric property,[8–10] and high carrier mobility.[11–13] Previous studies illustrated that PbSe properties could be additionally tuned by the morphology due to the quantum confinement effect.[12,14] Thus, PbSe quantum dots those are considered to be the zero-dimensional structure were widely used in solar energy applications.[11,15,16] The monolayer PbSe was also of great interest in the community not only because of the improved properties,[17] but also owing to the prediction of the two-dimensional (2D) topological insulator.[18,19] However, the reduce of thickness to reach the scale of 2D limit is facing more difficulties up to now. Unlike those layered semiconductors with interlayer van der Waals (vdW) interactions, PbSe in the bulk state possesses the so-called sodium chloride (NaCl)-type structure that belongs to the face-centered cubic lattice with homogeneous Pb–Se bonds in the whole crystal. It is therefore unlikely to achieve ultrathin PbSe simply through the mechanical exfoliation. Epitaxial growth, on the other hand, has been attempted to prepare ultrathin, smooth and thickness controlled PbSe. Various single crystal substrates were used to fabricate PbSe, but islands with large thickness rather than smooth films were obtained,[20,21] which indicates that the interaction between Pb and Se atoms within PbSe is larger than that to substrates.[22] Bilayer-thick PbSe was also prepared in large number of different mismatch layered compounds $(PbSe)_1(MSe_2)_n$, where M represents different transition metals.[23–25] In these systems, the inexistence of epitaxial relationship between PbSe and substrate helps the formation of crystallographically aligned ultrathin PbSe.[26] Recently, the formation of PbSe nanoplatelets was also achieved, extending the PbSe-based research as a quasi-2D platform.[7,27] A further approach by Shao *et al.* reported few layers of epitaxial PbSe on $SrTiO_3$ and revealed the strain affected electronic property of PbSe at the nanoscale.[28] However, the realization of ultrathin PbSe is still rarely reported experimentally, particularly on metal substrates. The direct contact between PbSe and metal substrate is significant when PbSe thin films are employed in the photothermal conversion for solar energy research[29] and the field-effect transistor for device applications.[30] As a result, the structural and electronic prop-

†Corresponding author. E-mail: li_zhang@hnu.edu.cn
‡Corresponding author. E-mail: zhqin@hnu.edu.cn

© 2022 Chinese Physical Society and IOP Publishing Ltd

erties of PbSe/metal at the atomic level require further research as well.

In this work, we studied the ultrathin PbSe synthesized via sequential molecular beam epitaxy (MBE) on Ag(111) by scanning tunneling microscopy and spectroscopy (STM/STS). It is found that the formation of ultrathin PbSe is only happened in the region that previously covered by Ag_5Se_2, revealing the selective reaction between Pb atoms and Ag_5Se_2 rather than AgSe. This selective behavior is further evidenced by the theoretical calculation where the cohesive energy of AgSe is prominently larger than that of Ag_5Se_2. Also, the quantity of deposited Pb was controlled to form PbSe with the different coverage. Specifically, the increased quantity of deposited Pb resulted in the improved quality of PbSe with larger and more uniform films. Further analysis reveals the bilayer feature of PbSe, which could be regarded as the realization of 2D limit. Differential conductance spectra acquired on PbSe exhibit a metallic feature due to the interaction between PbSe and Ag(111). Moreover, we carefully studied the moiré pattern originated from the lattice mismatch between PbSe and Ag(111). The formation of moiré lattice may indicate a partly decoupled PbSe, which will build up a foundation to explore the moiré modulated physics and benefit for device applications. Our approach provides a strategy for the selective synthesis of ultrathin PbSe on metal surfaces and suggests a 2D experimental system to explore PbSe-based opto-electronic and thermoelectric phenomena.

2. Materials and methods

2.1. Sample preparation and characterization

Ag(111) substrate was cleaned by repeated circles including Ar^+ bombardment (emission current: 1.2 μA) and subsequent annealing ($\sim$ 600 °C) in the preparation chamber of STM. Then, the processed Ag(111) was transferred to a home-built MBE chamber (base vacuum is better than 1×10^{-7} mbar) connected to the STM. Se (99.999%, Alfa Aesar) and Pb (99.999%, Alfa Aesar) were deposited successively on the Ag(111) substrate by a home-built evaporator. The exposure of fresh Ag(111) surface by Se, small and large amount of Pb was $\sim$ 17 L, $\sim$ 248 L and $\sim$ 370 L, respectively. The substrate was kept at room temperature during the Se and Pb deposition. Pt–Ir tips were used in the experiments, and calibrated on the Au(111) substrate before measurements.

All STM experiments were performed with an ultrahigh vacuum STM (Unisoku) at room temperature (base vacuum: $\sim 2\times10^{-10}$ mbar). STM images were acquired under constant current mode with sample biased. The differential conductance spectra were collected by a standard lock-in technique with 50 mV and 773 Hz modulation.

3. Calculation details

The density functional theory (DFT) calculations were performed using the Vienna *ab-initio* simulation package (VASP)[31] on the basis of the generalized gradient approximation (GGA) and the Perdew–Burke–Ernzerhof functional.[32] The energy cutoff was set to 450 eV and the Brillouin zone was integrated with a $20\times20\times1$ Γ centered k-point mesh. A vacuum of 20 Å was considered to neglect the artificial interaction between the monolayer with its image. All structures were fully relaxed with a force tolerance of 10^{-3} eV/Å, and the convergence threshold for energy minimization was selected to be 10^{-6} eV. The cohesive energy of the structure is calculated as

$$E_{\rm c}=\frac{E_{\rm monolayer}-E_X-E_{\rm Se}}{N_X+N_{\rm Se}},$$

where $E_{\rm monolayer}$ is the total energy of the monolayer, E_X is the energy of each Ag (Pb) atom obtained from its bulk, and $E_{\rm Se}$ is the energy of Se atom. N_X ($N_{\rm Se}$) denotes the number of metal (Se) atoms in the cell.

4. Results and discussion

The Se-deposited Ag(111) substrate was first annealed to form the flat surface, and two kinds of distinct surfaces different from pristine Ag(111) could be observed in the large-scale STM image (Fig. 1(a)). For the higher terrace, high-density grooves distribute and mainly compose triangle-like patterns, while for the lower terrace, the surface is relatively flat without any recognizable structural features. Zoom-in STM images associated to these two kinds of surfaces are shown with atomically resolution in Figs. 1(b) and 1(c), respectively. Two height profiles along the lattice vector of the two regions are shown in Fig. 1(d). It is clear that both structures can be assigned to the planar hexagonal lattice, but the lattice constant varies from each other. Thus, we can attribute the higher area in Fig. 1(a) to be Ag_5Se_2 with the lattice constant $\sim$ 0.8 nm, and the lower area to be AgSe with lattice constant $\sim$ 0.45 nm, which is consistent to the structure in literature.[33,34] It should be noted that the formation of higher and lower areas in Fig. 1 is due to the Ag steps. The thickness of Ag_5Se_2 and AgSe seems to be almost the same because they all exhibit the monolayer nature on the Ag(111) substrate.

After a small number of Pb atoms deposited on the $AgSe/Ag_5Se_2$ hybrid surface and subsequent annealing, the morphology in some region will change, as shown in the bottom part of Fig. 2(a). The high resolution STM image reveals the square-type lattice clearly marked by blue circles (Fig. 2(b)). Corresponding 2D fast Fourier transform (FFT) further proves the square-type feature, but there is a considerable deviation from the ideal square. Considering the room-temperature condition in STM scanning, we thus attribute such deformation to the thermal drift. The height profile containing

a few lattice periods was also acquired along one lattice vector, giving a lattice constant of ∼ 0.45 nm. This parameter along with the square-type feature significantly differs from that of Ag(111), AgSe or Ag_5Se_2 and is a strong evidence of the formation of PbSe according to reported results presenting a nearly identical structure.[28,35] We are also aware of some atomic-scale bright and dark sites randomly distributed within the lattice (Fig. 2(b)), which are probably the Pb adatoms and vacancies, respectively. We speculate that only small-area PbSe could assemble due to the insufficient Pb deposition. As a result, the small PbSe film is internally unstable and easily affected by nearby Ag–Se compounds. The process of forming PbSe is likely to be the spontaneous substitution reaction since the Pb element has a higher rank in the reactivity series of metals than Ag elements. Additionally, the substitution behavior prefers happening in the region that previously covered by Ag_5Se_2, which is concluded by the fact that the adjacent area of the PbSe domain contains some grooves standing for Ag_5Se_2 and there are very little significant changes in the region of AgSe. Theoretical calculations were performed to acquire the strength of relevant chemical bonds for estimating the reaction possibility. As can be seen in Table 1, the cohesive energy of Pb–Se bond in PbSe is larger than that of Ag–Se bond in AgSe and Ag_5Se_2, demonstrating that the PbSe thin film is a more stable layer from the energy point of view. These calculated results are similar to the reported dissociation energies of Pb–Se and Ag–Se bonds.[36] Moreover, the cohesive energy of Ag_5Se_2 is much smaller than that of AgSe, which reveals that Pb atoms prefer to interact with Ag_5Se_2 due to its less stability in comparison with the AgSe monolayer. Hence, one can reasonably expect the selective formation of PbSe in the Ag_5Se_2 region and the fixedness of the AgSe region.

Table 1. Calculated cohesive energies of AgSe, Ag_5Se_2 and PbSe.

	AgSe	Ag_5Se_2	PbSe
Cohesive energy (eV/atom)	–0.836	–0.380	–1.8

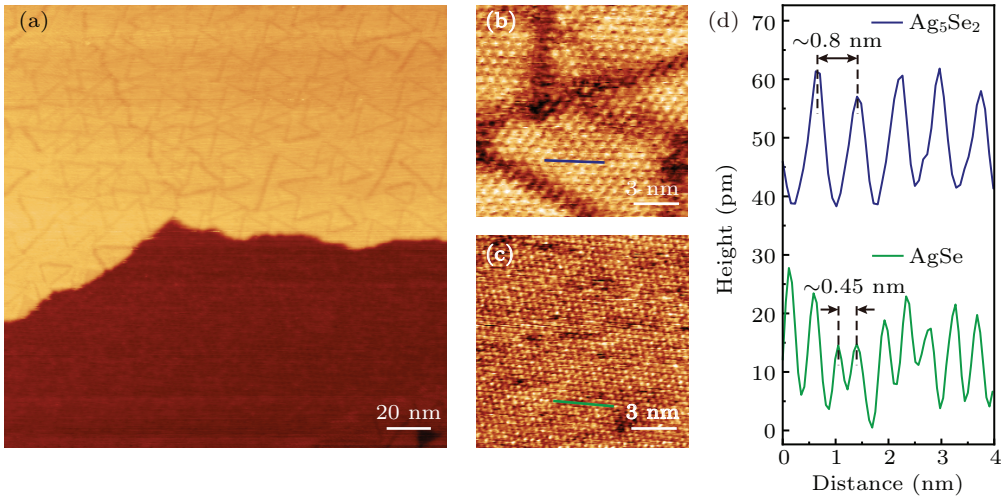


Fig. 1. (a) Large-scale STM image of AgSe and Ag_5Se_2 (1.2 V, 70 pA). (b) Atomically resolved STM image of Ag_5Se_2 (0.8 V, 70 pA). (c) Atomically resolved STM image of AgSe (0.8 V, 90 pA). (d) The height profiles along blue line in (b) and green line in (c). The blue line has been shifted for clarity.

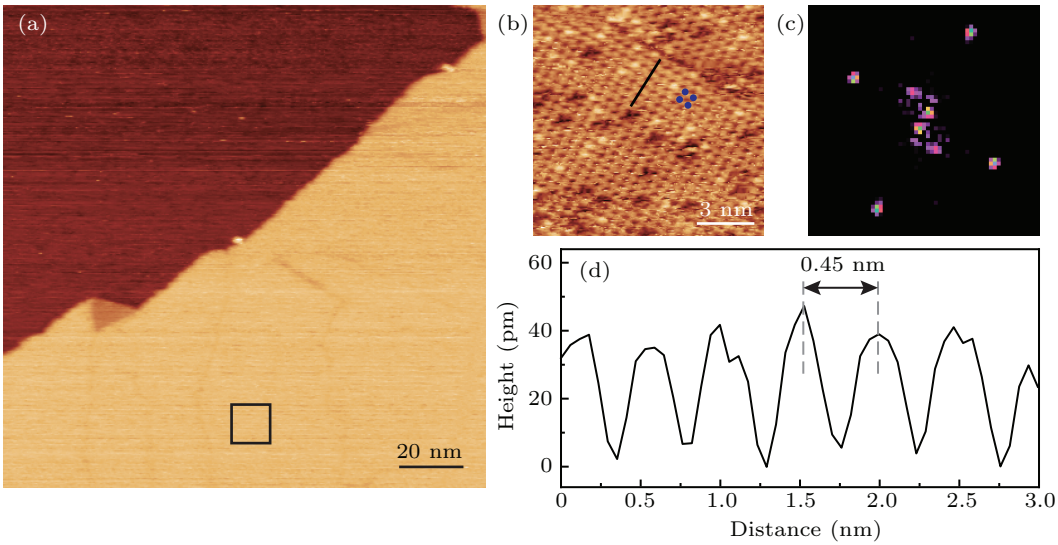


Fig. 2. (a) Large-scale STM image of surface after small amount of Pb deposition (1.2 V, 80 pA). (b) Atomically resolved STM image of the black square in (a) (0.7 V, 90 pA). Blue circles represent Pb atoms in PbSe. (c) 2D FFT of (b). (d) Height profile along black line in (b).

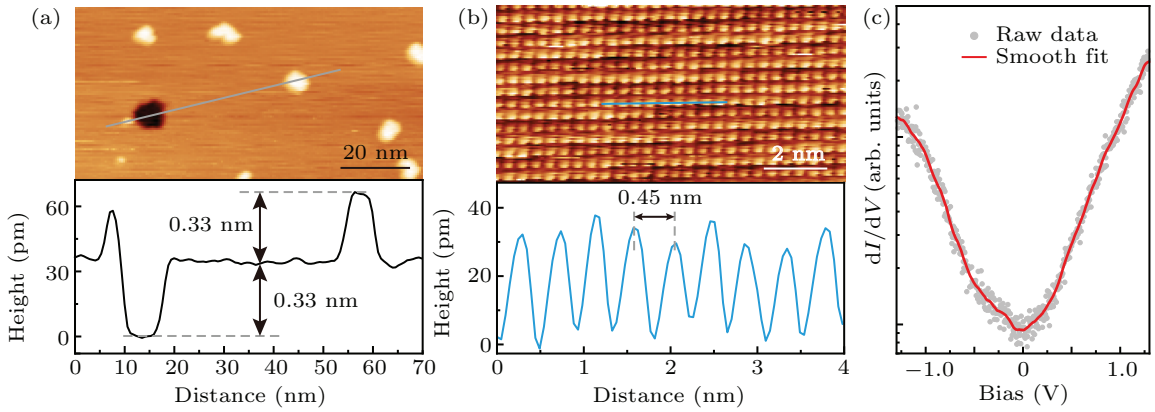


Fig. 3. (a) (Upper panel) Large-scale STM image of surface after large amount of Pb deposition (1.4 V, 60 pA). (Lower panel) Height profile along the grey line in the upper figure. (b) (Upper panel) Atomic-structure STM image of ultrathin PbSe (0.5 V, 200 pA). (Lower panel) Height profile along the light blue line in the upper figure. (c) Typical logarithm of $\mathrm{d}I/\mathrm{d}V$ spectrum acquired on PbSe.

The further amount Pb deposition and accompanying annealing were then carried out to synthesize the large-scale PbSe thin film. It is obvious that the area of ultrathin PbSe extended to the scale of at least 100 nm and covered certain parts of the surface, as illustrated in the upper panel of Fig. 3(a). Generally, the surface covered by PbSe is flat and uniform from the view of large scale, and one can only find a few bright spots and unhealed holes within a quite large area. Compared to situation with less Pb deposition, there is no Ag_5Se_2 region observed around the PbSe island, and the region of Ag_5Se_2 or AgSe even vanishes all over the surface, which may be ascribed to the coverage of Pb layers (see Fig. S1 in supporting information). The height profile across one hole and one spot was extracted from the STM image and displayed underneath. We found that the depth of holes and the height of spots share identical value (~ 0.33 nm), which is nearly the same to the thickness of PbSe with two atomic layers according to literatures.[28,35] Thus, it reveals the bilayer structure of ultrathin PbSe in our sample, and bright spots on PbSe could be small bilayer PbSe islands. The thickness of the synthesized PbSe nearly reaches the 2D limit in view of the instability of monolayer PbSe.[25] The zoom-in STM image with the atomic resolution explicitly shows a planar square structure (Fig. 3(b) upper panel) and the lattice constant is measured to be ~ 0.45 nm according to the height profile (Fig. 3(b) lower panel). Compared to Fig. 2(b), it can be confident to confirm the PbSe lattice with the defect-free feature. Hence, we can conclude that the increased Pb atoms and additional annealing improved the quality of PbSe films. The differential conductance spectrum ($\mathrm{d}I/\mathrm{d}V$) was acquired at the PbSe thin film and displayed in logarithmic coordinates (Fig. 3(c)). The typical metallic feature could be observed from the $\mathrm{d}I/\mathrm{d}V$ curve contrast to pristine ultrathin PbSe that belongs to semiconductors. The quenching effect of PbSe electronic states is the signature of a certain interaction between the Ag(111) substrate and PbSe thin films. The rest of the surface, however, is covered with the Pb-relevant structure and more STM images are shown in supporting information.

If we carefully explore the PbSe structure, an inconspicuous moiré lattice composed by series of short lines can be recognized in the relatively large area of PbSe thin films, as roughly labelled with green lines in Fig. 4(a). We could thus ascertain the basis vector and then found the hexagonal feature of the moiré lattice. The 2D FFT of Fig. 4(a) demonstrates the existence of two sets of lattices in the sample and they are grouped by circles with different colors (Fig. 4(b)). Except for the pronounced 4 reciprocal lattice points representing the square-type PbSe lattice, there are 6 reciprocal lattice points from the moiré lattice that can be observed. It is reasonable that the intensity of these points is weaker than those for PbSe lattice because of the bilayer structure for PbSe. To further resolve the structure, the corresponding inverse Fourier transform for these two groups of reciprocal lattices was carried out and reproduced the STM image (see detailed images in supporting information). Through the FFT pattern, it is concluded that the moiré lattice is formed by the mismatch between the square and hexagonal lattice with a small twisted angle.[37,38] Note that the twisted angle here only refers to one pair of selected basis vectors of PbSe and Ag(111) because of their different Bravais' lattice systems. Such twisted angle leads to the possibility of partly decoupling between the PbSe layer and substrate, rendering vdW interactions to some extent.

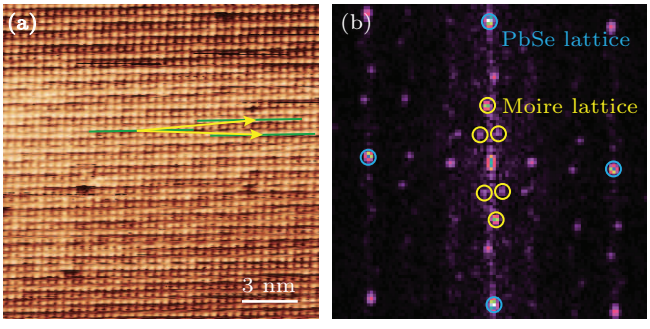


Fig. 4. (a) Atomically resolved STM image of PbSe with moiré pattern (0.5 V, 200 pA). Green lines indicate the nearby moiré lattice points and two yellow arrows represent basis vectors of moiré lattice. (b) 2D FFT of (a).

5. Conclusion

In summary, we have achieved the synthesis of high-quality ultrathin PbSe on Ag(111) via MBE methods evidenced by atomically resolved STM images exhibiting the PbSe-specific lattice. The formation of PbSe results from the selective reaction between Pb atoms and Ag_5Se_2 owing to its instability compared to AgSe. The increased quantity of accumulated Pb is found to affect the coverage of PbSe and additionally improve the quality with larger and more uniform films. Further analysis reveals the bilayer nature of PbSe, which is regarded as the realization of an ideal 2D PbSe. The dI/dV spectrum acquired on PbSe films presents a metallic feature owing to the interaction between PbSe and Ag(111). We also carefully studied the moiré pattern originated from the lattice mismatch between PbSe and Ag(111). The formation of moiré lattice may offer an opportunity to explore the physics modulated by the moiré potential and inspire potential applications for devices. Our approach demonstrates a MBE strategy for the selective synthesis of ultrathin PbSe on Ag(111) and suggests a 2D experimental system to explore PbSe-based opto-electronic and thermoelectric phenomena.

Acknowledgements

Project supported by the National Natural Science Foundation of China (Grant Nos. 12174096, 51772087, 51972106, 11904094, 11804089 and 12174095), the Strategic Priority Research Program of Chinese Academy of Sciences (Grant No. XDB30000000), and the Natural Science Foundation of Hunan Province, China (Grant Nos. 2019JJ50073 and 2021JJ20026). The authors acknowledge the financial support from the Fundamental Research Funds for the Central Universities of China.

References

[1] Geim A K and Novoselov K S 2007 *Nat. Mater.* **6** 183
[2] Radisavljevic B, Radenovic A, Brivio J, Giacometti V and Kis A 2011 *Nat. Nanotech.* **6** 147
[3] Wang Q H, Kalantar-Zadeh K, Kis A, Coleman J N and Strano M S 2012 *Nat. Nanotech.* **7** 699
[4] Zhang X, Qiao X F, Shi W, Wu J B, Jiang D S and Tan P H 2015 *Chem. Soc. Rev.* **44** 2757
[5] Pietryga J M, Werder D J, Williams D J, Casson J L, Schaller R D, Klimov V I and Hollingsworth J A 2008 *J. Am. Chem. Soc.* **130** 4879
[6] Nozik A J 2008 *Chem. Phys. Lett.* **457** 3
[7] Chen T R, Fan C, Zhou W C, Zou X M, Xu X, Wang S Y, Wan Q and Zhang Q L 2019 *Appl. Phys. Express* **12** 055005
[8] Parker D and Singh D J 2010 *Phys. Rev. B* **82** 035204
[9] You L, Liu Y, Li X, Nan P, Ge B, Jiang Y, Luo P, Pan S, Pei Y, Zhang W, Snyder G J, Yang J, Zhang J and Luo J 2018 *Energy Environ. Sci.* **11** 1848
[10] Tang S, Bai S, Wu M, Luo D, Wang D, Yang S and Zhao L D 2022 *Mater. Today Energy* **23** 100914
[11] Schaller R D and Klimov V I 2004 *Phys. Rev. Lett.* **92** 186601
[12] Liu Y, Gibbs M, Puthussery J, Gaik S, Ihly R, Hillhouse H W and Law M 2010 *Nano Lett.* **10** 1960
[13] Evers W H, Schins J M, Aerts M, Kulkarni A, Capiod P, Berthe M, Grandidier B, Delerue C, van der Zant H S J, van Overbeek C, Peters J L, Vanmaekelbergh D and Siebbeles L D A 2015 *Nat. Commun.* **6** 8195
[14] Moreels I, Lambert K, De Muynck D, Vanhaecke F, Poelman D, Martins J C, Allan G and Hens Z 2007 *Chem. Mater.* **19** 6101
[15] Beard M C, Midgett A G, Hanna M C, Luther J M, Hughes B K and Nozik A J 2010 *Nano Lett.* **10** 3019
[16] Semonin O E, Luther J M, Choi S, Chen H Y, Gao J B, Nozik A J and Beard M C 2011 *Science* **334** 1530
[17] Ul Haq B, AlFaify S, Ahmed R, Laref A, Mahmood Q and Algrafy E 2020 *Appl. Surf. Sci.* **525** 146521
[18] Wrasse E O and Schmidt T M 2014 *Nano Lett.* **14** 5717
[19] Liu J, Hsieh T H, Wei P, Duan W, Moodera J and Fu L 2014 *Nat. Mater.* **13** 178
[20] Zhao F, Ma J, Weng B, Li D, Bi G, Chen A, Xu J and Shi Z 2010 *J. Cryst. Growth* **312** 2695
[21] Strecker B N, McCann P J, Fang X M, Hauenstein R J, O'steen M and Johnson M B 1997 *J. Electron. Mater.* **26** 444
[22] Gannon R N, Choffel M M, Blackwood H R, Wolff N, Lotnyk A, Kienle L and Johnson D C 2022 *Z. Anorg. Allg. Chem.* e202200015
[23] Moore D B, Beekman M, Disch S, Zschack P, Häusler I, Neumann W and Johnson D C 2013 *Chem. Mater.* **25** 2404
[24] Grosse C, Alemayehu M B, Falmbigl M, Mogilatenko A, Chiatti O, Johnson D C and Fischer S F 2016 *Sci. Rep.* **6** 33457
[25] Cordova D L M, Fender S S, Hooshmand M S, Buchanan M R, Davis J, Kam T M, Gannon R N, Fischer R, Lu P, Hanken B E, Asta M and Johnson D C 2020 *Chem. Mater.* **32** 7992
[26] Cordova D L M, Kam T M, Fender S S, Tsai Y H and Johnson D C 2019 *Phys. Status Solidi A* **216** 1800896
[27] Galle T, Samadi Khoshkhoo M, Martin-Garcia B, Meerbach C, Sayevich V, Koitzsch A, Lesnyak V and Eychmüller A 2019 *Chem. Mater.* **31** 3803
[28] Shao Z, Zheng F, Zhang Z, Sun H, Li S, Yuan H, Li Q, Zhang P and Pan M 2019 *ACS Nano* **13** 2615
[29] Mane R S and Lokhande C D 2000 *Mater. Chem. Phys.* **65** 1
[30] Kim D K, Vemulkar T R, Oh S J, Koh W K, Murray C B and Kagan C R 2011 *ACS Nano* **5** 3230
[31] Kresse G and Furthmuller J 1996 *Phys. Rev. B* **54** 11169
[32] Perdew J P, Burke K and Ernzerhof M 1996 *Phys. Rev. Lett.* **77** 3865
[33] Lu J, Song S, Zhang S, Song Y, Cao Y, Wang Z, Huang L, Lu H, Zhang Y Y, Pantelides S T, Du S, Lin X and Gao H J 2022 *Nano Res.* **15** 6730
[34] Lu J, Gao L, Song S, Li H, Niu G, Chen H, Qian T, Ding H, Lin X, Du S and Gao H J 2021 *ACS Appl. Nano Mater.* **4** 8845
[35] Li X B, Guo P, Zhang Y N, Peng R F, Zhang H and Liu L M 2015 *J. Mater. Chem. C* **3** 6284
[36] Luo Y R 2007 *Comprehensive Handbook of Chemical Bond Energies*, 1st edn.
[37] Carnevali V, Marcantoni S and Peressi M 2021 *Comp. Mater. Sci.* **196** 110516
[38] Wu Q, Bagheri Tagani M, Zhang L, Wang J, Xia Y, Zhang L, Xie S Y, Tian Y, Yin L J, Zhang W, Rudenko A N, Wee A T S, Wong P K J and Qin Z 2022 *ACS Nano* **16** 6541